

Effects of serrated grain boundaries on the crack growth in austenitic heat-resisting steels during high-temperature creep

MANABU TANAKA, HIROSHI IIZUKA, FUMIO ASHIHARA

Department of Mechanical Engineering for Production, Mining College, Akita University, 1-1, Tegatagakuen-cho, Akita 010, Japan

The effect of serrated grain boundaries on creep crack growth is investigated using an austenitic 21Cr-4Ni-9Mn steel principally at 700°C. The relationship between the microstructure of specimens and the crack growth behaviour is discussed. The creep crack growth rate in the specimens with a surface notch is relatively reduced by serrated grain boundaries especially in the early stage of crack growth. The life of crack propagation in the specimens with serrated grain boundaries is longer compared with that of the specimens with straight grain boundaries. It is confirmed in the surface crack growth of smooth round bar specimens crept at 700°C that serrated grain boundaries are effective in retarding the growth of a grain-boundary crack less than about 4×10^{-4} m long, and that this effect decreases with increasing crack length. It is suggested that crack deflection due to serrated grain boundaries caused a decrease in the stress intensity factor of the grain-boundary crack and resulted in a decrease of the crack growth rate in the steel. The crack arrest at the deflection points and the circumvention of crack path on the serrated grain-boundaries may also contribute to the retardation of the grain-boundary crack growth during creep. Further, it is deduced from the experimental results on the notched specimens that the creep fracture is caused by the linkage of the main crack to many microcracks and voids on the grain-boundary at 900°C.

1. Introduction

Serrated grain boundaries are effective in improving the creep rupture strength [1-5] and the low-cycle fatigue strength [6, 7] of heat-resisting alloys at high temperatures. It was confirmed in a previous study on austenitic 21Cr-4Ni-9Mn steel [8] that the creep rupture strength was improved by serrated grain boundaries at high temperatures above 600°C. The grain-boundary sliding in specimens was relatively reduced by serrated grain boundaries. It was also found that serrated grain boundaries were effective in retarding the initiation of grain-boundary cracks in this steel.

It is known from the analysis based on the fracture mechanics [9-12] that the crack deflection decreases the stress intensity factor of the crack. The crack path also becomes longer when the crack propagates on the wavy path [10]. The retardation of grain-boundary crack growth by serrated grain boundaries may be explained by similar reasons, but details of the strengthening mechanism remain unknown.

In this study, the creep crack growth is examined on an austenitic 21Cr-4Ni-9Mn steel with serrated grain boundaries and with normal straight grain boundaries, of equal matrix hardness principally at 700°C. The relation between parameters of metallography and fracture mechanics and grain-boundary crack growth is discussed.

2. Experimental procedure

The basic components of austenitic 21Cr-4Ni-9Mn steel used in this study were 0.54%C, 0.39%N, 21.10%Cr, 4.07%Ni and 9.74%Mn. The steel bars of 16 mm diameter were heat treated in order to precipitate carbides at grain boundaries and in the interior of grains to obtain specimens with serrated grain boundaries (steel S) and those with normal straight grain boundaries (steel N) with the same matrix hardness (about 320 H_v) (Fig. 1) [8]. Steel S had a grain-boundary segment length of about 2×10^{-5} m and steel N had a grain-boundary length of about 5.7×10^{-5} m; both specimens had the same grain diameter of about 9.9×10^{-5} m.

Creep experiments were performed using single

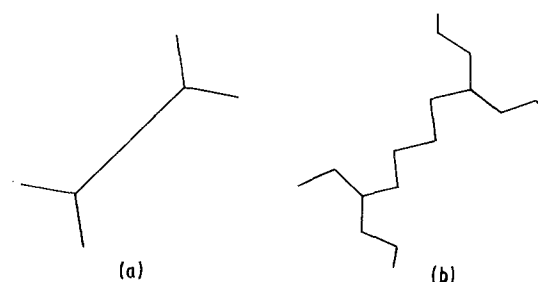


Figure 1 Schematic illustration of grain-boundary configurations of specimens. (a) Straight grain boundary; (b) serrated grain boundary.

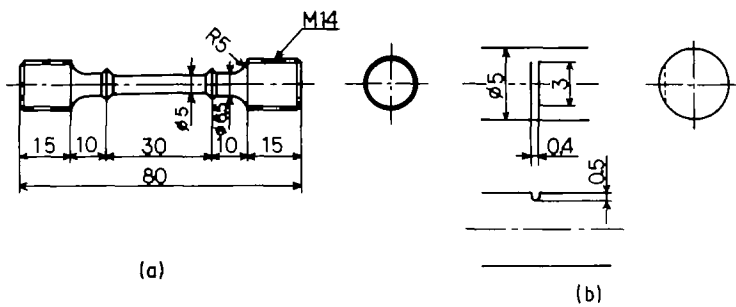


Figure 2 The geometry of specimens used for creep and creep rupture experiments. (Dimensions in mm.) ϕ = diameter.

level-type creep-rupture equipments at 700 and 900°C in air. Fig. 2 shows the geometry of creep specimens used in this study. Smooth round bar specimens with 30 mm gauge length and 5 mm diameter were used for creep rupture and surface crack growth experiments (Fig. 2a), and those with a shallow transverse notch were employed for crack growth experiments (Fig. 2b). The crack length of the specimen was measured by examining directly the specimen surface or the extracted surface replica using optical microscopy after interrupting creep tests and cooling the specimens to room temperature. The notch opening displacement, which was an increase in width of notch, was also measured. The specimen was then loaded again after heating to the test temperature. All the stresses described in this paper are gross stresses, and the size of surface crack length and crack depth includes that of the notched part.

The geometry of a crack was readily known from heat tinting of the creep ruptured specimens at 700°C, and the ratio of surface length to depth of a crack (aspect ratio) was experimentally obtained. The crack depth of the surface notched specimens could be calculated from the surface length of a crack using this aspect ratio. The crack growth rate was obtained by plotting crack length (or crack depth) against time, t , and reading the inclination of a tangent of the curve plotted.

3. Results and discussions

3.1. Effect of grain-boundary configuration on the creep crack growth in the notched specimens at 700°C

Fig. 3 shows the relation between depth and surface length of a crack observed on the smooth round

bar specimens creep ruptured under stresses in the range from 196 to 294 MPa at 700°C. All the creep cracks examined in this study are nucleated and propagate on grain boundaries, irrespective of the grain-boundary configuration of the specimens. The product of specimen radius, $d/2$, and angle, θ , gives the surface crack length. The ratio of crack depth, a , to specimen diameter, d , i.e. a/d , increases with an increase in angle θ (or surface crack length), while the ratio R/d shows a constant value of 0.679 for both specimens with serrated grain boundaries and those with straight grain boundaries. Thus, the value of $(2a/d\theta)$ gives the aspect ratio of the crack.

Fig. 4 shows the increment of surface crack length and the notch opening displacement during creep at 700°C. In specimens with a surface notch, the time of crack propagation in the specimens with serrated grain boundaries is longer than that in the specimens with straight grain boundaries, the time to crack initiation at notch root in the former is not so long compared with the latter. This may indicate that the stress concentration in the vicinity of the notch promotes the grain-boundary crack initiation even in specimens with serrated grain boundaries. The notch opening displacement, as well as the increment of crack length, increases acceleratedly with time in both the specimens at 196 MPa, but the notch opening occurs more gradually than the crack growth at 167 MPa. Thus, the geometry of a crack was not necessarily maintained constant throughout the time of crack growth.

Fig. 5 shows a short crack emanating from the notch root on the specimen surface crept under a stress of 196 MPa at 700°C. Cracks are indicated by arrows in the figure. The crack is nucleated on the

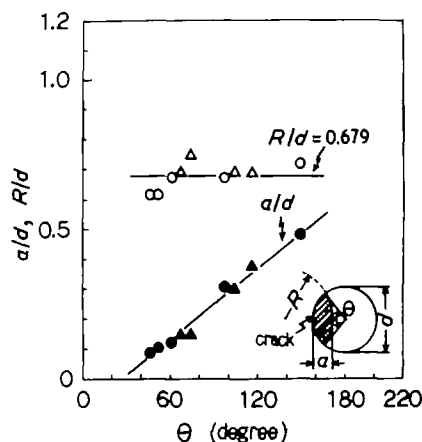


Figure 3 The geometry of grain-boundary cracks observed on the smooth round bar specimens creep ruptured at 700°C. R/d : (○) steel S, (△) steel N. a/d : (●) steel S, (▲) steel N.

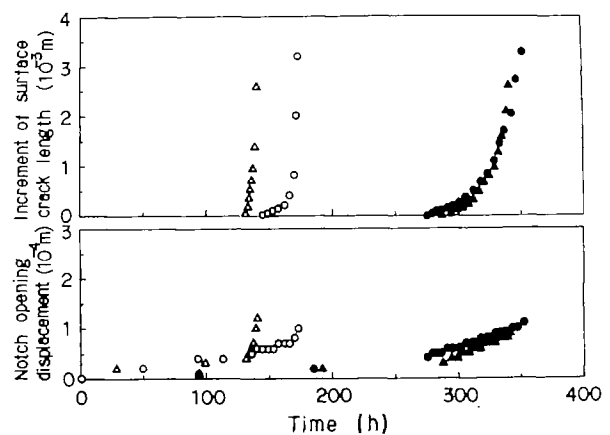


Figure 4 The increment of surface crack length and the notch opening displacement in the specimens during creep at 700°C, at (○, △) 196 MPa, (●, ▲) 167 MPa for (○, ●) steel S, (△, ▲) steel N.

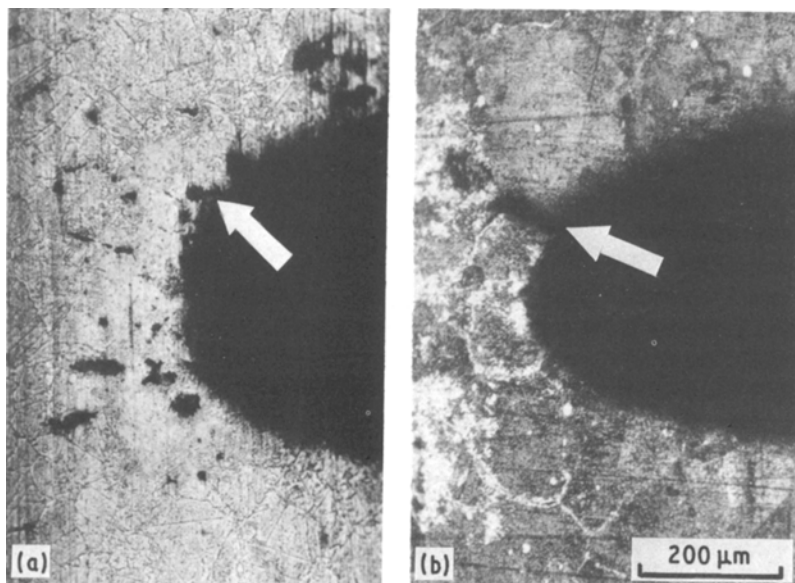


Figure 5 The grain-boundary crack growing from the notch root on the specimen surface crept under a stress of 196 MPa at 700°C. (a) Steel S (at 145 h), (b) steel N (at 131 h).

grain boundary both in specimens with serrated grain boundaries and those with straight grain boundaries. The crack depth is confirmed on some surface notched specimens. The specimens are cut parallel to the longitudinal direction after propagating the surface crack to a given size. Fig. 6 shows a crack growing from the notch root to the inside of the specimen. The grain-boundary crack propagates macroscopically in the direction normal to the tensile axis both in specimens with serrated grain boundaries and those with straight grain boundaries, but the crack path is wavy in the microscopic scale because the crack propagates on the grain boundaries. The crack depth calculated from the surface crack length and the aspect ratio of the crack (Fig. 3) agrees with the actual crack depth within an accuracy of about 10% for specimens crept at 700°C.

Fig. 7 shows the relation between surface crack growth rate and surface crack length in the surface notched specimens during creep at 700°C. The surface crack growth rate of the specimens with serrated grain boundaries is relatively lower than that of the specimens with straight grain boundaries under stresses of 167 and 196 MPa when the crack is short, but the former approaches the latter with increasing crack length.

The crack depth and the crack growth rate to the inside of the specimens can be obtained from the results of surface crack propagation experiments using the relation between crack depth and surface crack length (Fig. 3). Fig. 8 shows the relation between crack growth rate and stress intensity factor, K_I , during creep at 700°C. The maximum K_I value for the specimens with a surface crack is given using variables shown in Fig. 3 by [13]

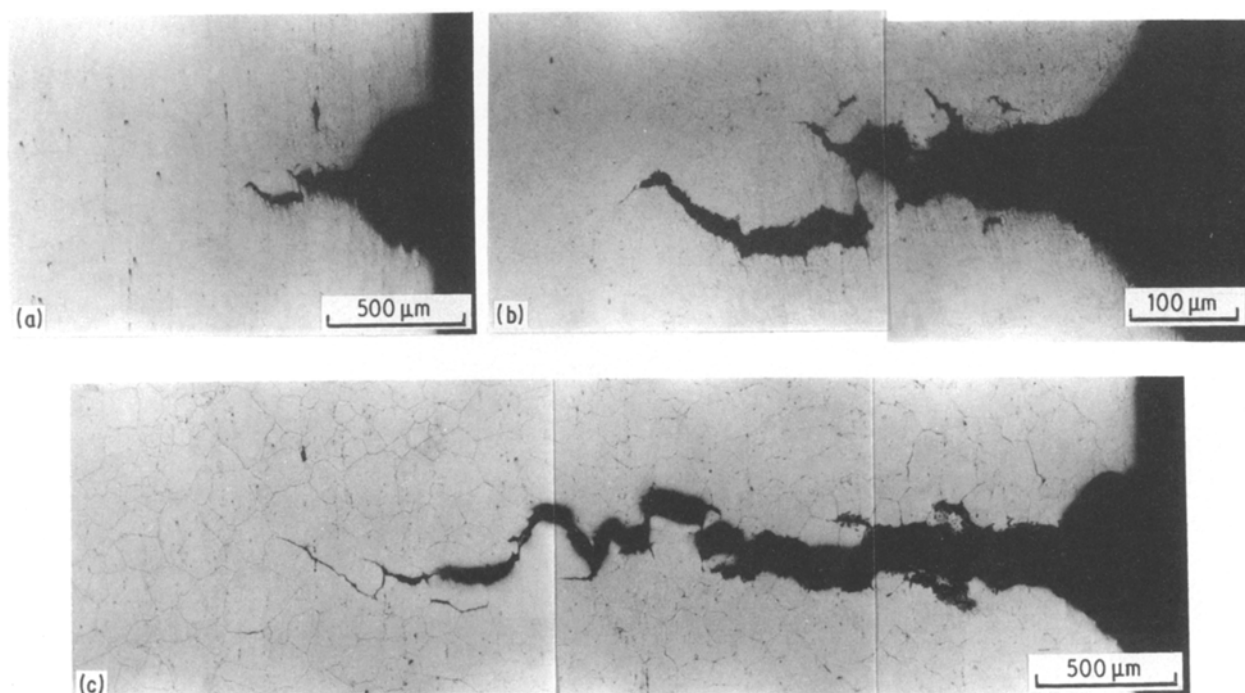


Figure 6 The grain-boundary crack growing from the notch root towards the inside of a specimen during creep under a stress of 196 MPa at 700°C. (a) Steel S ($2l = 3.88 \times 10^{-3}$ m); (b) steel S, enlarged micrograph of (a); (c) steel N ($2l = 5.89 \times 10^{-3}$ m), where $2l$ is the length of the surface crack.

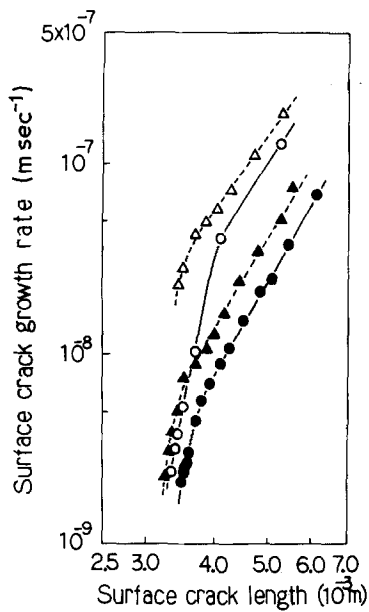


Figure 7 The relation between growth rate and length of surface crack in the notched specimens during creep at 700°C, at (Δ, ○) 196 MPa, (▲, ●) 167 MPa for (○, ●) steel S, (Δ, ▲) steel N.

$$K_I = \sigma_g (\pi a)^{1/2} \{ 1.12 + (0.30/d - 1.85/R)a - [6.63/d^2 - 10.25/(Rd)]a^2 + [23.13/d^3 - 18.75/(Rd^2)]a^3 \} \quad (1)$$

$(a/d \leq 0.4 \text{ and } R \geq 0.5d)$

where σ_g is the gross stress. It is known that serrated grain boundaries are effective in retarding the crack growth to the inside of specimens when the macroscopic K_I value is small (i.e. when the crack size is small), but that the effect diminishes with an increase of K_I (i.e. an increase of crack depth).

Kitagawa and Yuuki [9] have reported that the K_I of a deflected crack depends on a ratio of deflected portion to total length of crack, and that K_I decreases with increasing proportion of the deflected part of

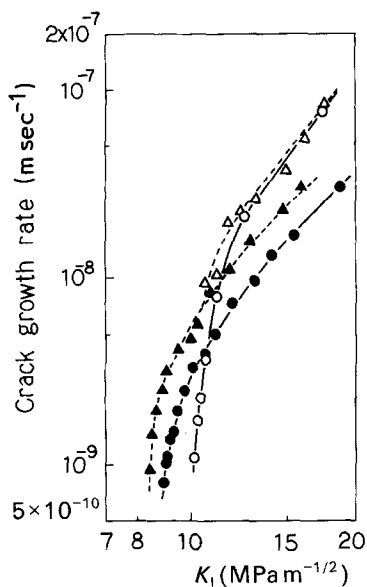


Figure 8 The relation between crack growth rate and K_I in the notched specimens during creep at 700°C, and (○, Δ) 196 MPa, (●, ▲) 167 MPa for (○, ●) steel S, (Δ, ▲) steel N.

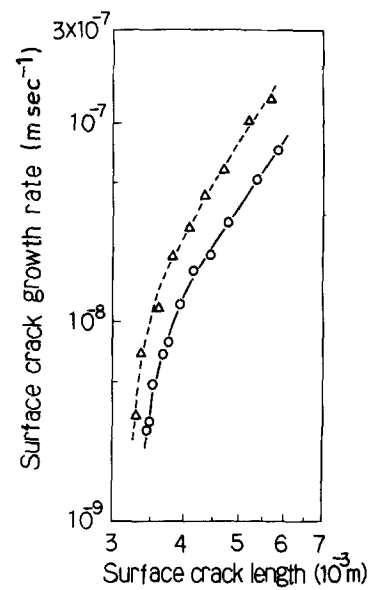


Figure 9 The relation between growth rate and length of surface crack in the notched specimens during creep under a stress of 27.4 MPa at 900°C, for (Δ) steel N, (○) steel S.

the crack even for the same projected crack length on the original crack trajectory. Ishida [11] has shown that the stress intensity factor of a serrated crack normal to the tensile axis is almost constant, independently of the number of serrations. Suresh [10] has also obtained similar results on the growth of a deflected crack. Further, the circumvention of the crack path by serrated grain boundaries may also retard the crack growth by lengthening the crack path [10]. In the specimen with serrated grain boundaries, the grain-boundary crack is deflected both on the serrated grain boundaries and at the grain-boundary triple junctions. The effect of serrated grain boundaries may be reduced by the crack deflection of a larger scale at the grain-boundary triple junctions when the grain-boundary crack becomes longer than several grain diameters in length. Therefore, it is predicted that the effect of serrated grain boundaries will diminish with crack growth. This coincides with the experimental results. The same results are also obtained on the growth of surface microcracks in the smooth round bar specimens in the next section.

Fig. 9 shows the relation between the growth rate and the length of a surface crack in specimens crept under a stress of 27.4 MPa at 900°C. The surface crack growth rate is reduced by serrated grain boundaries even at 900°C. Fig. 10 shows the cracks observed at the notch root of a specimen with serrated grain boundaries and that with straight grain boundaries when the surface crack length is about 6×10^{-3} m. Many microcracks and voids are visible in the vicinity and at the notch root of both the specimens. However, the specimen surface is covered with a thick oxide layer produced by severe oxidation at this temperature, and the diameter of the specimen is reduced by more than 10% after removing this. Thus, the true crack depth of the main crack is not known in these specimens. The creep rupture may be caused by the linkage of the main crack with many microcracks and voids on grain boundaries in both the specimens at 900°C.

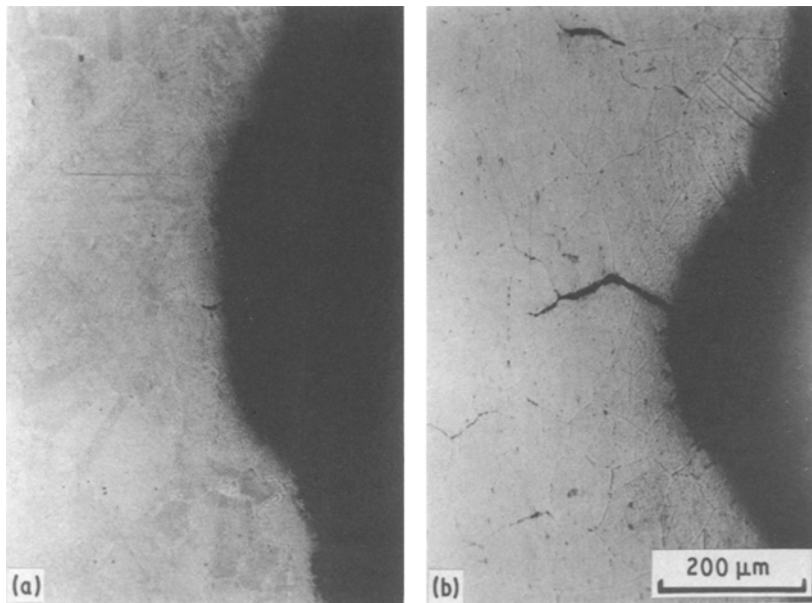


Figure 10 The grain-boundary crack observed at the notch root of the notched specimens crept under a stress of 27.4 MPa at 900°C (the surface crack length is about 6×10^{-3} m) (a) Steel S, (b) Steel N.

3.2. Growth of microcracks in the smooth bar specimens during creep

The effect of serrated grain boundaries on the initiation and growth of microcracks was also investigated using smooth bar specimens during creep at 700°C. Fig. 11 shows the relation between growth rate of the largest microcrack and its length on the specimen surface during creep under a stress of 196 MPa at 700°C. The crack growth rate of the specimen with serrated grain boundaries is apparently lower than that of the specimen with straight grain boundaries when the length of the microcrack is less than about 4×10^{-4} m, while the difference in crack growth rate between these specimens virtually diminishes beyond this crack size. It is also found in both the specimens that the largest crack observed in the current step of examination is not always the same as that examined in the previous step and that the largest crack does not necessarily grow fastest. This implies that the crack

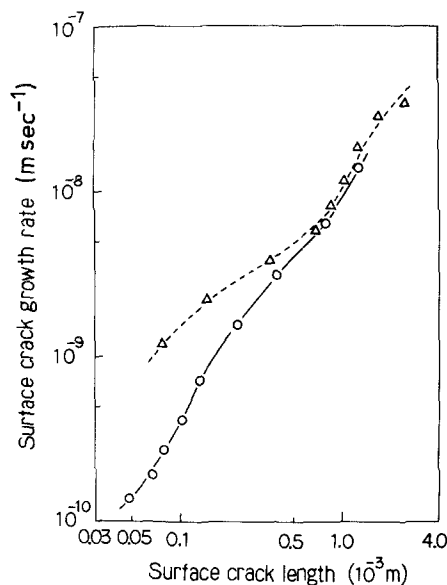


Figure 11 The relation between growth rate of the largest surface microcrack and its length in the smooth bar specimens during creep under a stress of 196 MPa at 700°C, for (Δ) steel N, (\circ) steel S.

grows intermittently with time and that the retardation of crack growth may also be caused by the crack arrest at the inflection points on the serrated grain boundaries and at the grain-boundary triple junctions.

Fig. 12 shows the surface microcrack in the early stage of crack growth on specimens crept under a stress of 196 MPa at 700°C. Arrows in the figure indicate microcracks. The microcrack observed on the specimen with serrated grain boundaries is deflected, while that found on the specimens with straight grain boundaries is almost linear. As mentioned above, it has been reported by other investigators that the stress intensity factor of the deflected crack is lower than that of a linear crack [9–12], and that its value decreases with increasing proportion of the deflected part of the crack to the remainder [9]. The grain-boundary crack in the specimens with serrated grain boundaries has a very large proportion of crack deflection in the early stages of crack growth, as shown in Fig. 12. In addition, the crack growth may be retarded by lengthening of the crack path through circumvention of the crack and also by crack arrest at the inflection points on the serrated grain boundaries. The experimental results of the growth of surface microcracks also indicate that the retardation of crack growth by serrated grain boundaries is especially effective in the early stages of crack growth, and that its effect decreases with crack growth.

The inhibition of grain-boundary sliding and the occurrence of ductile grain-boundary fracture by serrated grain boundaries may also play some role in retarding the grain-boundary crack growth during creep [8], but it is still not clear in this study.

4. Conclusions

The effect of serrated grain boundaries on creep crack growth was investigated using austenitic 21Cr–4Ni–9Mn steel principally at 700°C. The relationship between the growth of a grain-boundary crack and the grain-boundary configuration of the specimens has been discussed. The results obtained are summarized as follows.

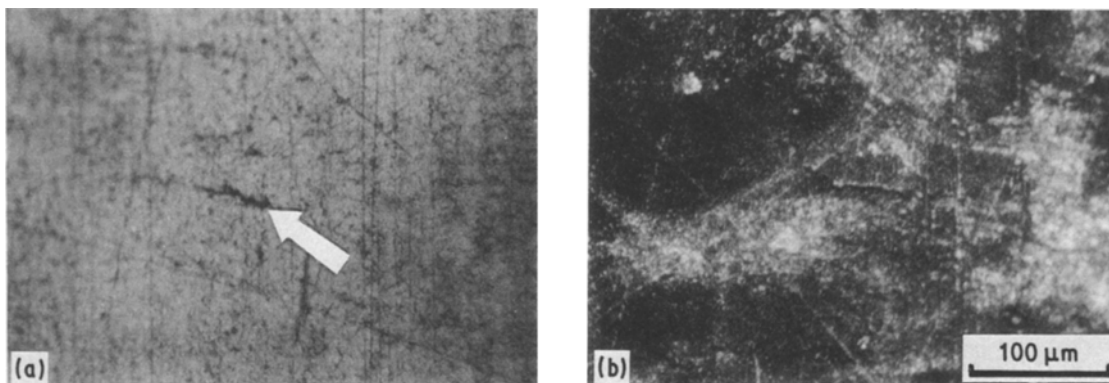


Figure 12 The surface microcracks observed in the early stage of crack growth in specimens crept under a stress of 196 MPa at 700°C. (a) Steel S, (b) steel N.

1. The serrated grain boundary was effective in retarding the growth of a grain-boundary crack during creep. Its effect was especially large in the early stages of crack growth and diminished with increasing crack length. It was concluded that the retardation of crack growth was caused by the crack deflection on serrated grain boundaries which resulted in a decrease of stress intensity factor of crack, the circumvention of crack path and crack arrest at the inflection points on the serrated grain boundaries. The effectiveness of serrated grain boundaries may have been reduced by the crack deflection at the grain-boundary triple junctions when the crack size became large.

2. All the creep cracks were formed on grain boundaries, irrespective of the grain-boundary configuration of the specimens. In the surface notched specimens crept at 700°C, the crack was initiated at the notch root and propagated macroscopically in the direction normal to the tensile direction. The crack growth rate in the specimens with serrated grain boundaries was much lower than that in the specimens with straight grain boundaries especially when the crack length was short. The microcracks and voids were observed on the grain boundary in the vicinity of and at the notch root of the surface notched specimens at 900°C. The grain-boundary fracture was probably caused by the linkage of the main crack with these microcracks and voids at this temperature.

3. The growth rate of the largest surface microcrack on smooth round bar specimens with serrated grain boundaries was lower than that on specimens with straight grain boundaries at 700°C when the crack length was less than 4×10^{-4} m, but the difference in

the crack growth rate virtually diminished beyond this crack size.

References

1. M. YAMAZAKI, *J. Jpn Inst. Metals* **30** (1966) 1032.
2. W. BETTERIDGE and A. W. FRANKLIN, *J. Inst. Metals* **85** (1956-57) 473.
3. T. SAGA, O. MIYAGAWA, M. KOBAYASHI and D. FUJISHIRO, *Trans. Iron Steel Inst. Jpn* **58** (1972) 859.
4. M. YAMAMOTO, O. MIYAGAWA, M. KOBAYASHI and D. FUJISHIRO, *ibid.* **63** (1977) 1848.
5. M. TANAKA, O. MIYAGAWA, T. SAKAKI and D. FUJISHIRO, *Tetsu to Hagané* **65** (1979) 939.
6. J. C. RUNKLE and R. M. PELLOUX, in "Micromechanisms of Low-Cycle Fatigue in Nickel-Based Superalloys at Elevated Temperatures", edited by J. T. Fong, ASTM STP 675 (American Society for Testing and Materials, Philadelphia, 1979) p. 501.
7. H. IIZUKA, M. TANAKA, O. MIYAGAWA and D. FUJISHIRO, in "Proceedings of Fourth JIM International Symposium on Grain Boundary Structure and Related Phenomena", held in Minakami, Gunma Prefecture, edited by Y. Ishida *et al.* (Japan Institute of Metals, Sendai, Japan, 1985) p. 851.
8. M. TANAKA, O. MIYAGAWA, T. SAKAKI, H. IIZUKA, F. ASHIHARA and D. FUJISHIRO, *J. Mater. Sci.* **23** (1988) 621.
9. H. KITAGAWA and R. YUUKI, *Trans. Jpn Soc. Mech. Eng.* **41-346** (1975) 1641.
10. S. SURESH, *Metall. Trans.* **14A** (1983) 2375.
11. M. ISHIDA, *Trans. Jpn. Soc. Mech. Eng.* **45-392** (1979) 306.
12. V. VITEK, *Int. J. Fracture* **13** (1977) 481.
13. A. KIUCHI, M. AOKI, M. KOBAYASHI and K. IKEDA, *Tetsu to Hagané* **68** (1982) 1830.

Received 9 November 1987

and accepted 1 March 1988